Electronic Supplementary Material (ESI) for Organic & Biomolecular Chemistry

--Supporting Information--

Between Two Worlds: a Comparative Study on *In Vitro* and *In Silico* Inhibition of Trypsin and Matriptase by Redox-Stable SFTI-1 Variants at Near Physiological pH

Olga Avrutina,[a] Heiko Fittler,[a] Bernhard Glotzbach,[a] Harald Kolmar,[a] and Martin Empting[a,*]

[a] *Clemens-Schöpf Institute of Organic Chemistry and Biochemistry, Technische Universität Darmstadt, Petersenstr. 22, 64287 Darmstadt, Germany.*

Table of Contents

Experimental Procedures

Instrumentation

Analytical HPLC was conducted using a Varian 920-LC system equipped with a Phenomenex Hypersil 5u BDS C18 LC column (150 x 4.6 mm, 5 µm, 130 Å). Semi-preparative RP-HPLC was performed on a Varian modular system comprising a PrepStar 218 Solvent Delivery Module, a ProStar 410 HPLC AutoSampler and a ProStar 325 Dual Wavelength UV-Vis HPLC Detector using a YMC J'sphere ODS-H80 C-18 LC column (250 x 20 mm, 4 µm, 8 nm). The eluent system for analytical and semi-preparative HPLC consisted of eluent A (0.1% aq. TFA) and eluent B (90 % aq. acetonitrile containing 0.1% TFA).
ESI mass spectra were recorded using a Shimadzu LCMS-2020 equipped with a Phenomenex Jupiter 5u C4 LC column (50 x 1 mm, 5 µm, 300 Å). The eluent system consisted of eluent A (0.1% aq. formic acid, LC-MS grade) and eluent B (acetonitrile containing 0.1% formic acid, LC-MS grade).
Fast protein liquid chromatography (FPLC) was conducted using an ÄKTApurifier (Amersham Pharmacia Biotech).

General Fmoc-SPPS Procedures

Peptides were synthesized on a Liberty 12-channel automated peptide synthesizer coupled with a Discover SPS microwave peptide synthesizer platform (CEM) using the Fmoc strategy. Amino acids were attached by double or triple coupling employing 4 eq of the corresponding amino acid, 4 eq of 2-(1H-benzotriazol-1-yl)-1,1,3,3-tetramethyluronoium hexafluorphosphate (HBTU) and 8 eq of *N*,*N*-diisopropylethylamine (DIEA), or in case of cysteine 3-4 eq of 2,4,6-trimethylpyridine (collidine). Arginine and cysteine were coupled using a two-step microwave program: 1. RT, 0 W, 25 min; 2. 75 °C, 25 W, 0.5 min (Arg) and 1. RT, 0 W, 2 min; 2. 50 °C, 25 W, 4 min (Cys), respectively. All other amino acids were coupled using a standard microwave program: 75 °C, 21 W, 5 min.
Fmoc deprotection was achieved in two steps by reaction with 20% piperidine in DMF at 75 °C, 42 W for 0.5 min (initial deprotection) followed by a second deprotection step with 20% piperidine in DMF at 75 °C, 42 W for 3 min.

Compounds 2 and 4–6

Synthesis and characterization of compounds **2** and **4**–**6** have already been described in detail in reference 13 from the main text.

SFTI-1 (1)

The linear precursor of **1** was synthesized on chlorotrityl resin preloaded with Fmoc-Gly (0.59 mmol/g) at 0.25 mmol scale according to the automated Fmoc-SPPS protocol described above. The peptide was cleaved from the resin under conservation of side chain protection using 5 mL of a mixture of acetic acid, DCM, and methanol (50:40:10, v/v/v) for 2 h at ambient temperature. The solvents were evaporated. To the resulting yellow oil *n*-hexan was added and then evaporated. This step was repeated three times. The residue was dissolved in 20 mL H_2O/CH_3CN (1:1, v/v) and lyophilized. 30 mg (0.025 mmol) of the linear peptide were dissolved in 30 mL dry DMF, and 4.4 mg HOBT (5 eq), 17 mg (5 eq) benzotriazol-1-yl-oxytripyrrolidinophosphonium hexafluorophosphate (PyBOP) as well as 11.3 µL (10 eq) DIEA were added for backbone macrocyclization. After 16 h of reaction, additional portions of HOBT (4.4 mg, 5 eq), PyBOP (17 mg, 5 eq), and DIEA (11.3 µL, 10 eq) were added and the reaction mixture was stirred overnight at ambient temperature. The solvent was evaporated and the protecting groups were removed by acidolytic cleavage using TFA/H_2O/anisole/triethylsilane (TES) (47:1:1:1, v/v/v/v) and a small amount of dithiothreitol (DTT). The reaction mixture was shaken for 3 h at ambient temperature with subsequent by precipitation and washing (3×) with 30 mL methyl *tert*-butyl ether (MTBE) to yield the crude monocyclic peptide. Oxidative disulfide formation was conducted in 100 mM $(NH_4)_2CO_3$ aq (pH = 8.6) at 1 mg peptide/mL dilution. After complete conversion, the solvent was removed *in vacuo* to yield the crude peptide. Chromatographic isolation by RP-HPLC yielded 4.5 mg of pure **1** (11.9 %).
RP-HPLC: Rt = 15.5 min (18 % acetonitrile over 2 min followed by 18→40.5 % acetonitrile in 0.1 % TFA over 20 min at flow rate 1 mL/min). ESI-MS: m/z: $[M+H]^+$ obsd. = 1514.6 (calc = 1513.7), $[M+2H]^{2+}$ obsd. = 757.8 (calc = 757.4), $[M-H]^-$ obsd. = 1511.8 (calc = 1511.7).

[Ala^3(&^{1}),Ala^{11}(&^{2})]SFTI-1[1,14][(&^{1}-1,5-[1,2,3]triazolyl-&^{2})] (3)

The amino acid sequence Fmoc-Aza-Thr(tBu)-Lys(Boc)-Ser(tBu)-Ile-Pro-Pro-Ile-Pra-Phe-Pro-Asp(tBu) was assembled on an AmphiSpheres 40 HMP resin (0.4 mmol/g, Varian/Agilent) at 0.125 mmol scale using the automated microwave-assisted Fmoc-SPPS procedure described above. Loading of the resin with Fmoc-Asp(tBu)-OH was conducted by triple coupling 2 eq AA, 2 eq 2-(1H-7-azabenzotriazol-1-yl)-1,1,3,3-tetramethyluronoium hexafluorphosphate (HATU), 4 eq DIEA and two-step microwave program (1. 60 °C, 30 W, 45 min, 2. 75 °C, 20 W, 5 min). Fmoc-Aza-OH and Fmoc-Pra-OH were attached using double coupling of 2 eq AA, 2 eq HATU, 4 eq DIEA, and two-step microwave program (1. 60 °C, 30 W, 45 min, 2. 75 °C, 20 W, 5 min). On-support ruthenium(II)-catalyzed macrocyclization of linear resin-bound precursor was conducted as previously reported (reference 12 from the main text). *N*-terminal sequence Gly-Arg(Pbf) was assembled using double coupling for each amino acid (4 eq aa, 3.9 eq HBTU, 8 eq DIEA) and microwave

irradiation (50 °C, 30 W, 30 min). The peptide resin was dried and subjected to acidolytic cleavage using TFA/H_2O/anisole/TES (47:1:1:1, v/v/v/v). Ether precipitation, washing, and subsequent purification *via* semi-preparative HPLC yielded 2.1 mg macrocyclic peptide **3** (1.37 µmol, 1.1 % according to the initial loading of the resin).

RP-HPLC: Rt = 16.2 min (18 % acetonitrile over 2 min followed by 18→40.5 % acetonitrile in 0.1 % TFA over 20 min at flow rate 1 mL/min). ESI-MS (m/z) $[M+2H]^{2+}$ obsd. = 768.56 (calc = 767.9), $[M+3H]^{3+}$ obsd. = 512.85 (calc = 512.8), $[M-H]^-$ obsd. = 1533.29 (calc = 1532.8). IR (cm^{-1}) 3424, 2924, 1652, 1538, 1451, 1203, 1132.

Inhibition Assays

Kinetic curves were recorded by monitoring the absorption of the corresponding samples in 96-well plates (NUNC, flat bottom, clear) at 405 nm in intervals of 60 sec over 30 min at RT using the Tecan GENios microplate reader. All experiments were performed in triplicate. Trypsin from bovine pancreas (Sigma) or matriptase were standardized by active-site titration with *p*-nitrophenyl-*p*'-guanidinobenzoate (NPGB) in phosphate buffered saline (PBS: 137 mM NaCl, 2.7 mM KCl, 10.0 mM Na_2HPO_4, 1.76 mM KH_2PO_4, pH 7.4).

The normalized residual proteolytic activity v/v_0 of trypsin against the chromogenic substrate Boc-QAR-*p*NA (250 µM, Bachem) at different concentrations of bicyclic and monocyclic SFTI-1 analogues **1**-**6** [I] was determined for ~ 0.5 nM (trypsin) or 0.9 nM (matriptase) active enzyme ([E]) in aqueous buffer (50 mM Tris/HCl, 150 mM NaCl, 0.01% Triton X-100, 0.01% sodium azide, pH 7.6 or 8.5). The apparent inhibition constants (K_i^{app}) were calculated by fitting the Morrison equation for tight binding inhibitors (1) onto the resulting kinetic data with the Marquardt-Levenberg algorithm of SigmaPlot 11.

Determination of Michaelis-Menten Constant (K_M) for Boc-QAR-pNA against Matriptase

The initial reaction rate (v_i) of the proteolytic degradation of Boc-QAR-*p*NA (Bachem) by matriptase (1 nM) was determined for a series of concentrations ($[S]_i$) of the chromogenic substrate (1000-75 µM for pH 7.6 and 1000-50 µM for pH 8.5). The Michaelis-Menten constant (K_M) was calculated *via* Lineweaver-Burk plot (reciprocal initial reaction rate 1/vi versus the reciprocal substrate concentration $1/[S]_i$) and linear regression of the resulting data. The experiment was performed in triplicate yielding K_M as 236.8±56.1 µM (pH 7.6) and 66.6±16.0 µM (pH 8.5) (arithmetic mean, standard deviation given as error).

Transformation of Equation (2) into Equation (3)

$$\frac{v}{v_o} = \frac{([E]-[I]-K_i^{app})+\sqrt{([I]+K_i^{app}-[E])^2+4K_i^{app}[E]}}{2[E]} \qquad (2)$$

$$\frac{v}{v_o} = \frac{2[E]-2[E]+[E]-[I]-K_i^{app}+\sqrt{([I]+K_i^{app}-[E])^2+4K_i^{app}[E]}}{2[E]} \qquad (8)$$

$$\frac{v}{v_o} = \frac{2[E]}{2[E]} + \frac{-[E]-[I]-K_i^{app}+\sqrt{([I]+K_i^{app}-[E])^2+4K_i^{app}[E]}}{2[E]} \qquad (9)$$

$$\frac{v}{v_o} = 1 - \frac{([E]+[I]+K_i^{app})-\sqrt{([I]+K_i^{app}-[E])^2+4K_i^{app}[E]}}{2[E]} \qquad (10)$$

$$\frac{v}{v_o} = 1 - \frac{([E]+[I]+K_i^{app})-\sqrt{[I]^2+(K_i^{app})^2+[E]^2+2K_i^{app}[I]-2[E][I]-2K_i^{app}[E]+4K_i^{app}[E]}}{2[E]} \qquad (11)$$

$$\frac{v}{v_o} = 1 - \frac{([E]+[I]+K_i^{app})-\sqrt{[I]^2+[E]^2+(K_i^{app})^2+2K_i^{app}[E]+2K_i^{app}[I]+2[E][I]-2[E][I]-2[E][I]}}{2[E]} \qquad (12)$$

trinomial theorem

$$\frac{v}{v_o} = 1 - \frac{([E]+[I]+K_i^{app})-\sqrt{([E]+[I]+K_i^{app})^2-4[E][I]}}{2[E]} \qquad (3) \quad \blacksquare$$

Propagation of Errors for $\Delta_B G^{exp}$

$\Delta_B G^{exp}$ for trypsin and matriptase complexes of compounds **1**–**6** were calculated from *in vitro* K_i using equation (7). The error of $\Delta_B G^{exp}$ ($\Delta\Delta_B G^{exp}$) was calculated by propagation of errors of K_i (ΔK_i) as follows:

$$(\Delta\Delta_B G^{exp})^2 = \left|\frac{\partial \Delta_B G^{exp}}{\partial K_i}\right|^2 (\Delta K_i)^2 \qquad (13)$$

$$\Delta\Delta_B G^{exp} = \sqrt{\left|\frac{\partial \Delta_B G^{exp}}{\partial K_i}\right|^2 (\Delta K_i)^2} \qquad (14)$$

Finally, differentiation of $\Delta_B G^{exp}$ with respect to K_i yields equation (15).

$$\Delta\Delta_B G^{exp} = \sqrt{\left|\frac{-RT}{K_i}\right|^2 (\Delta K_i)^2} \qquad (15)$$

In Silico Methods

Instrumentation

All *in silico* experiments were performed on an Intel® Core™ i7-2600 workstation using 8 virtual cores.

Graphical Content

Graphical content for Figures 1, 3, 6, S1, and S2 was generated with YASARA (www.yasara.org) and POVRay (www.povray.org).

Force Field Parameters for Triazoles within Peptidomimetics 3–6

Each triazolyl moiety was modeled manually into residue 11 of peptidomimetics **3**–**6** and then connected *via* a single C-C bond to residue 3 as depicted in Scheme S1.

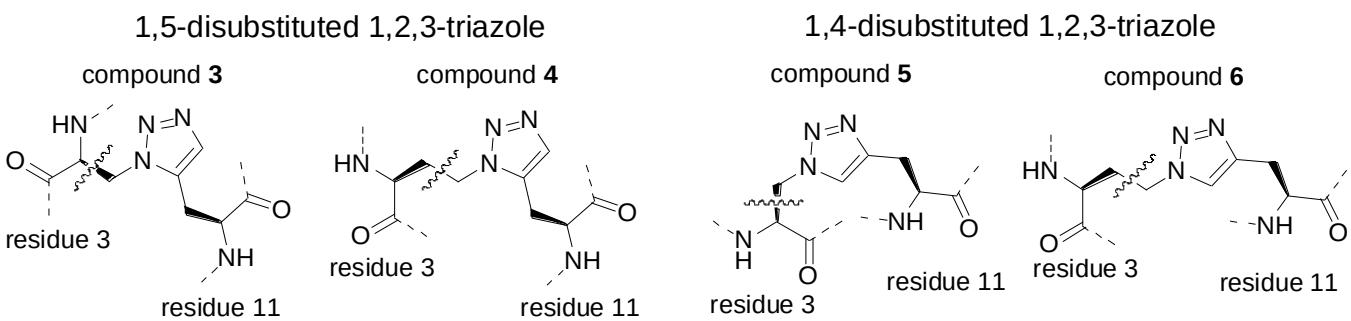

Scheme S1. Affiliation of atoms within triazolyl moieties to respective residues within compounds **3**–**6**.

Supporting Figures

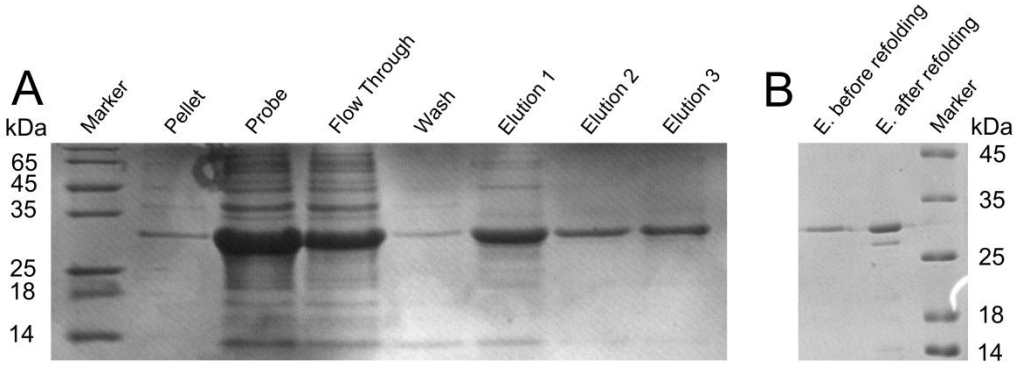

Fig S1 (A) SDS-PAGE of fractions collected using an immobilized metal ion affinity chromatography (IMAC) column upon purification of human matriptase I under denaturing conditions. Inclusion bodies were produced in *E. coli* BL21-DE3-CodonPlus-RP with the expression vector pET42dest-His-hMatI(cd)596-855 and dissolved in buffer 1 (50 mM Tris-HCl, 100 mM NaCl, 1 mM 2-mercaptoethanol, 6 M urea) after cell disruption. Elution was achieved using buffer 2 (50 mM Tris-HCl, 100 mM NaCl, 1 mM 2-mercaptoethanol, 4.5 M urea). (B) SDS-PAGE of human matriptase I before and after refolding. Refolding was achieved by 3 steps of dialysis for 4-6 hours: 1× against refolding buffer 1 (50 mM Tris-HCl, 100 mM NaCl, 1 mM 2-mercaptoethanol, 3 M urea) and then 2× against refolding buffer 2 (50 mM Tris-HCl, 100 mM NaCl, 1 mM 2-mercaptoethanol).

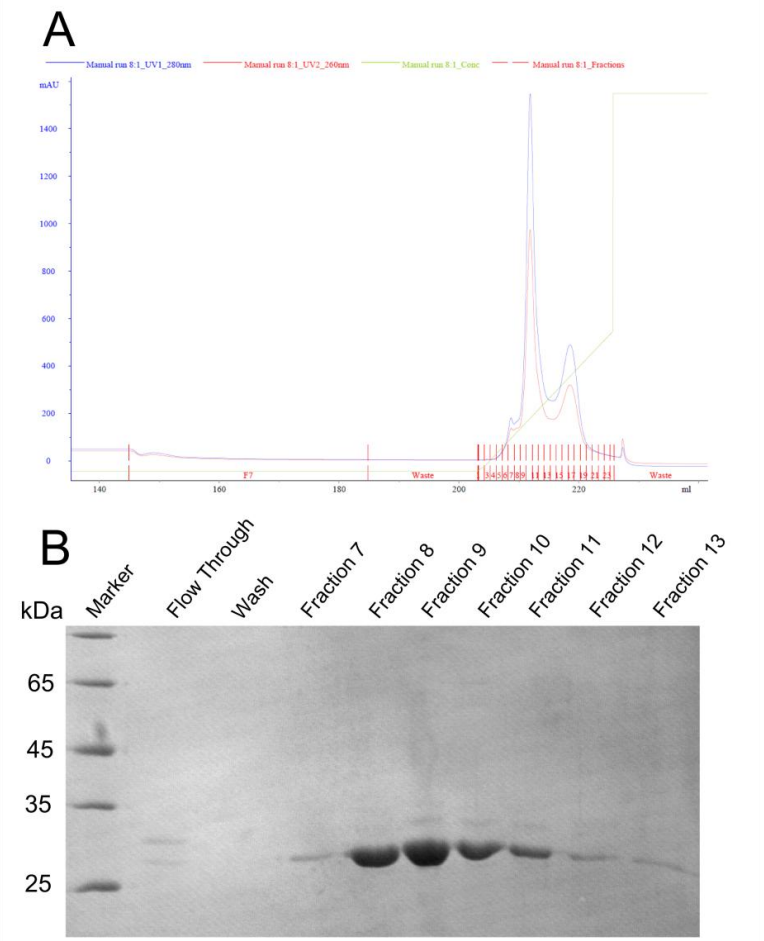

Fig S2 (A) FPLC trace of refolded/autocatalytically activated human matriptase I using an anion-exchange chromatography column (HiTrap Q HP, GE Healthcare) with detection at 260 nm (red) and 280 nm (blue). Sodium chloride was removed from protein solution before FPLC *via* dialysis against 50 mM Tris-HCl pH 8. Target protease was eluted by an increasing sodium chloride gradient 0→500 mM in 50 mM Tris-HCl (green) at a flow rate of 1 mL/min. Collected fractions are indicated (red lines). (B) SDS-PAGE of the collected fractions.

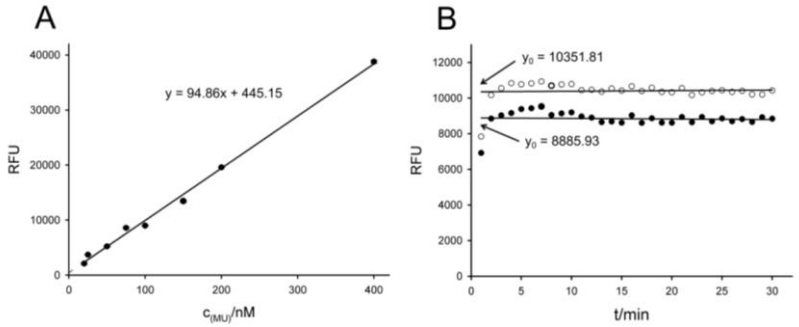

Fig S3 Analysis of proteolytic activity of the purified matriptase. (A) Calibration curve (linear regression) for fluorophor 4-methylumbelliferone (MU; Sigma) recorded at 465 nM using eight different concentrations and an excitation wavelength of 360 nM. (B) Active-site titration of purified matriptase using fluorogenic 4-methylumbelliferyl-*p*-guanidinobenzoate (MUGB; 1µM; Sigma) in buffer (50 mM Tris/HCl, 150 mM NaCl, 0.01% (v/v) Triton X-100, 0.01% (w/v) sodium azide, pH 7.6). Mean values of two independent measurements over 30 minutes (white circle 250 nM and black circle 200 nM of purified protease) y-intercept of linear regression is given. Protease activity was determined as 43 % of total protein concentration.

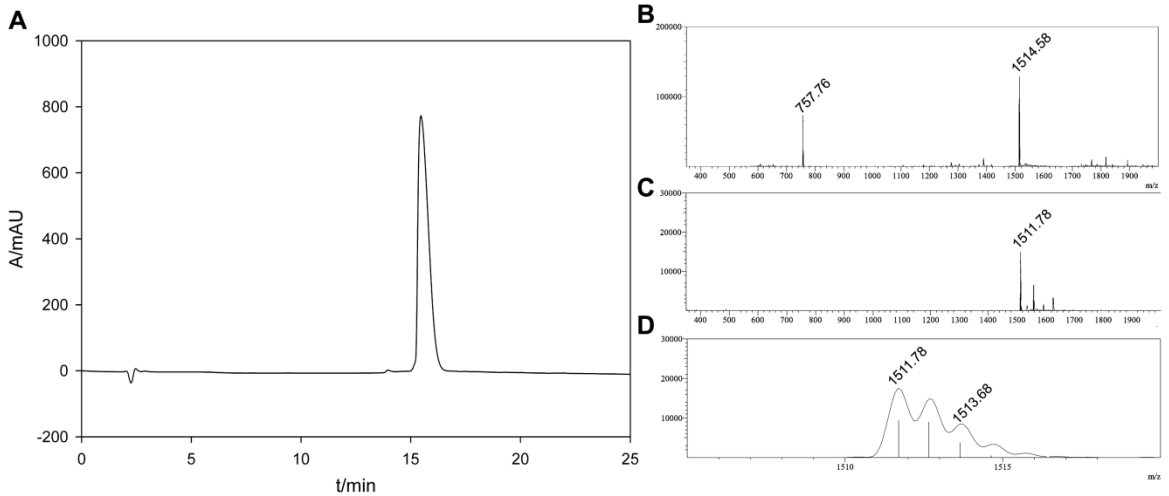

Fig S4 (A) RP-HPLC trace of bicyclic SFTI-1 (**1**). Conditions: 18 % acetonitrile over 2 min followed by 18→40.5 % acetonitrile in 0.1 % TFA over 20 min at flow rate 1 mL/min. (B) ESI mass spectrum of **1** (positive polarization). (C) ESI mass spectrum of **1** (negative polarization). (D) Section (m/z 1505-1520) of negative ESI mass spectrum showing isotopic pattern of $[M-H]^-$ signal of **1**.

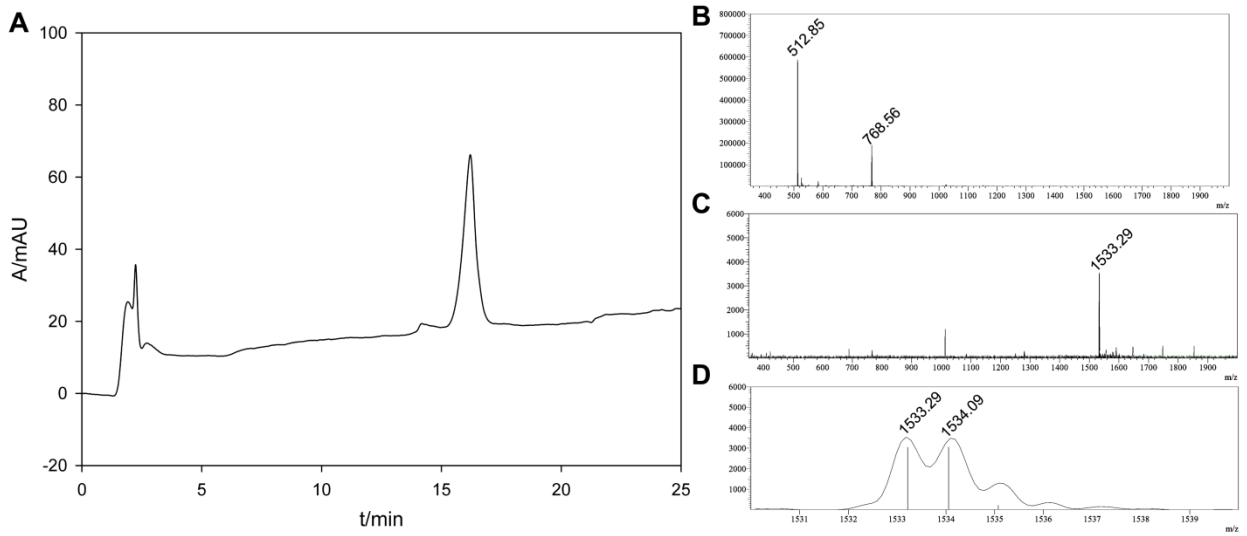

Fig S5 (A) RP-HPLC trace of peptidomimetic inhibitor (**3**). Conditions: 18 % acetonitrile over 2 min followed by 18→40.5 % acetonitrile in 0.1 % TFA over 20 min at flow rate 1 mL/min. (B) ESI mass spectrum of **3** (positive polarization). (C) ESI mass spectrum of **3** (negative polarization). (D) Section (m/z 1530-1540) of negative ESI mass spectrum showing isotopic pattern of $[M-H]^-$ signal of **3**.

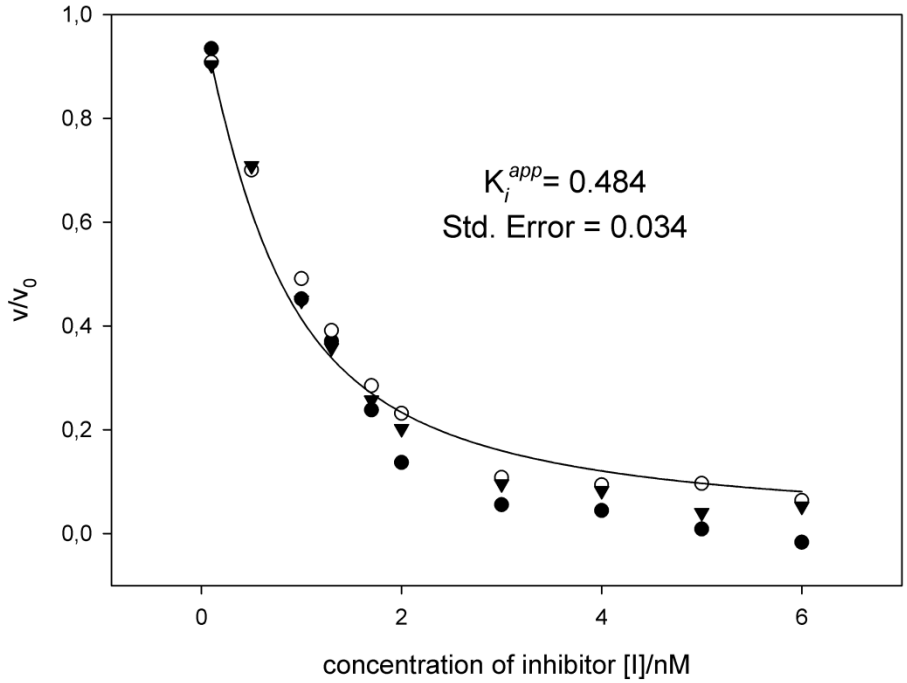

Fig. S6 Plottet kinetic data for the inhibition of the proteolytic activity of trypsin by bicyclic inhibitor **1** and resulting curve for the global non-linear fit of equation (3) onto the three sets of experimental data (1: white circle, 2: black circle, 3: black triangle). Determined apparent inhibition constant K_i^{app} and the standard error of the fit are given in nM.

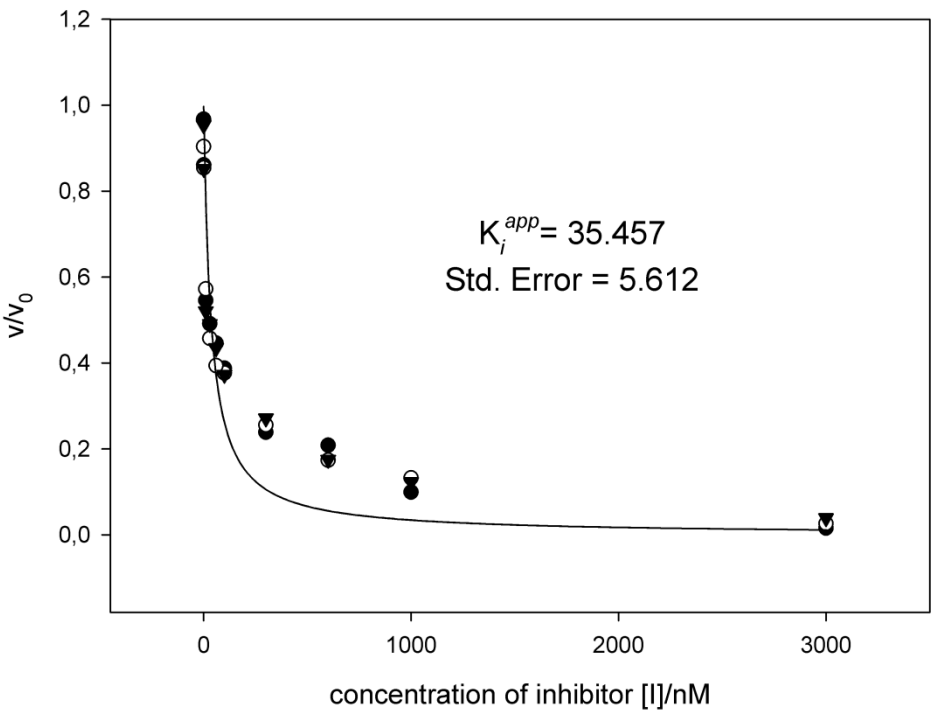

Fig. S7 Plottet kinetic data for the inhibition of the proteolytic activity of trypsin by peptidomimetic inhibitor **3** and resulting curve for the global non-linear fit of equation (3) onto the three sets of experimental data (1: white circle, 2: black circle, 3: black triangle). Determined apparent inhibition constant K_i^{app} and the standard error of the fit are given in nM.

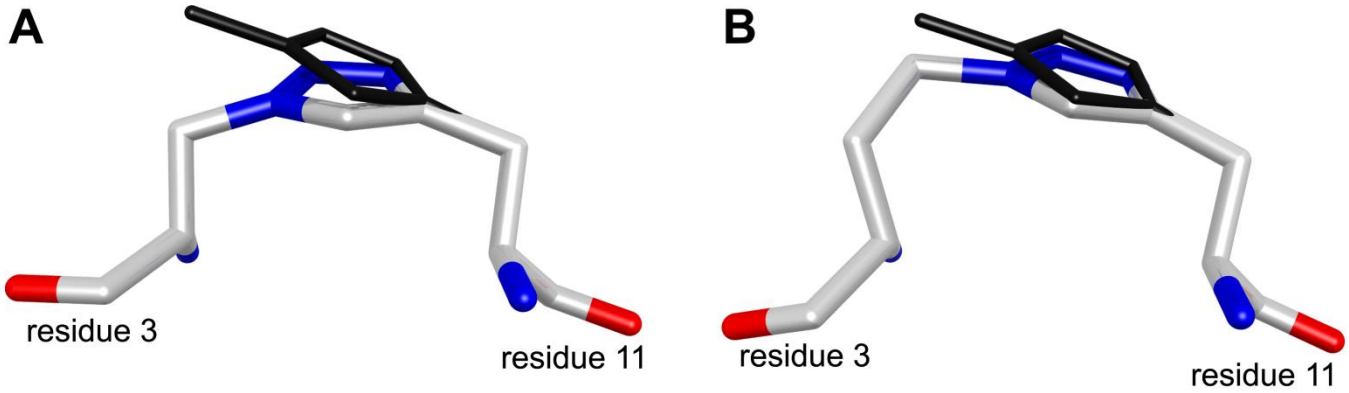

Fig S8 Bent triazolyl structures within the macrocyclization motif of compounds **5** (A) and **6** (B) resulting after modeling and a singular energy minimization step in an overlay with a corresponding planar triazole structure (thin, black). Blue: nitrogen, red: oxygen, white: carbon, hydrogen omitted for clarity, only residues 3 and 11 are shown.

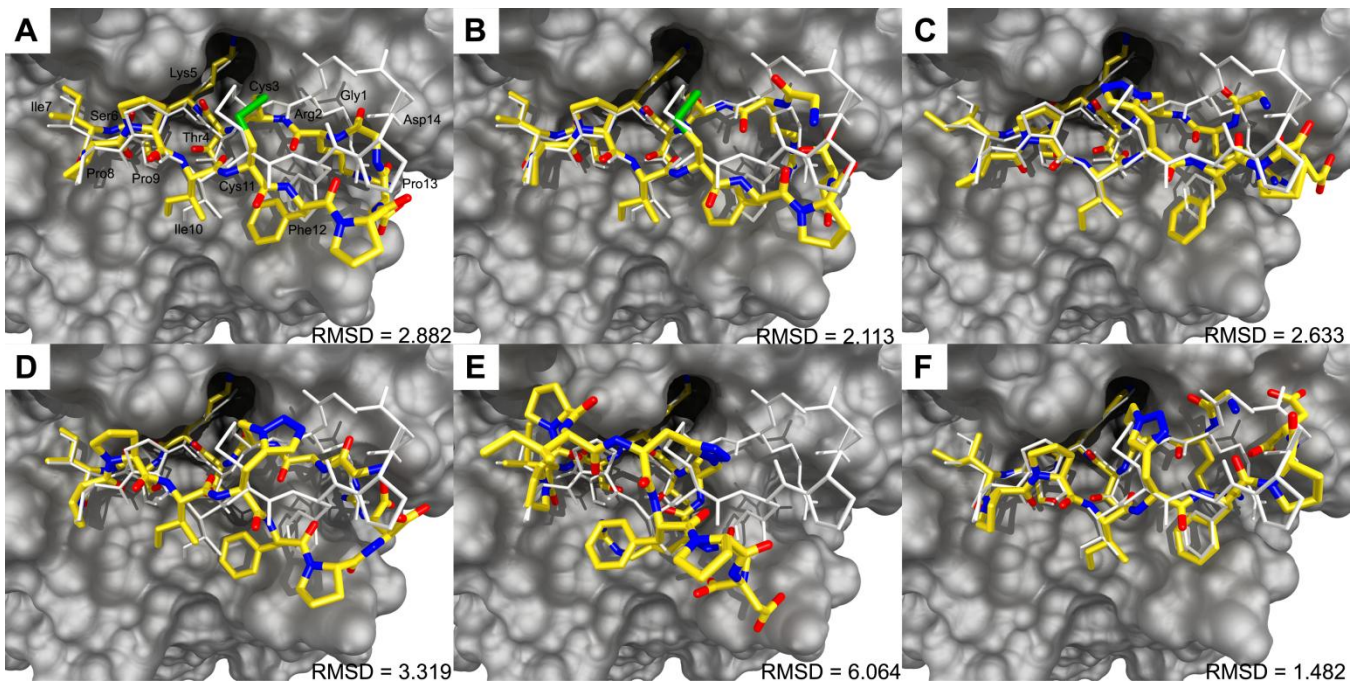

Fig. S9 Predicted structures of compounds **1** (A), **2** (B), **3** (C), **4** (D), **5** (E), and **6** (F) in complex with trypsin (grey surface) as an overlay with reported crystal structure 1SFI (reference 2 from the main text) (white sticks). Blue: nitrogen, green: sulfur, red: oxygen, yellow: carbon, hydrogen is omitted for clarity. Measured RMSD values for inhibitor backbones compared to 1SFI are given in Å.

Supporting Tables

Table S1 Determined K_i for compounds **1**-**6** against trypsin at pH 7.6 using equations (1) and (4 or 5)[a,b] (K_i^1), (2) and (6) (K_i^2), as well as (3) and (6) (K_i^3).

Entry	K_i^1/nM	K_i^2/nM	K_i^3/nM
1	0.06[a]	0.07	0.07
2	0.21[a]	0.21	0.21
3	5.08[b]	5.07	5.07
4	0.34[a]	0.34	0.34
5	272.74[b]	272.72	272.73
6	106.12[b]	106.09	106.09

[a]Equation (5) was used. [b]Equation (4) was used.

Table S2 Determined K_i for compounds **1**-**6** against matriptase at pH 7.6 using equations (1) and (4) (K_i^1), (2) and (6) (K_i^2), as well as (3) and (6) (K_i^3).

Entry	K_i^1/nM	K_i^2/nM	K_i^3/nM
1	1100.1	1099.9	1099.9
2	702.8	702.5	702.5
3	1236.9	1236.7	1236.7
4	12930.0	12929.1	12929.8
5	285258.8	284749.5	284748.4
6	94092.1	94084.5	94096.2

Table S3 Determined K_i for compounds **1** & **2** against matriptase at pH 8.5 using equations (1) and (4) (K_i^1), (2) and (6) (K_i^2), as well as (3) and (6) (K_i^3).

Entry	K_i^1/nM	K_i^2/nM	K_i^3/nM
1	147.5	147.4	147.4
2	100.3	100.2	100.2

Table S4 Assignment of atom types for investigated 1,5-disubstituted 1,2,3-triazoles and 1,4-disubstituted 1,2,3-triazoles.

Structure	Atom	Atom type
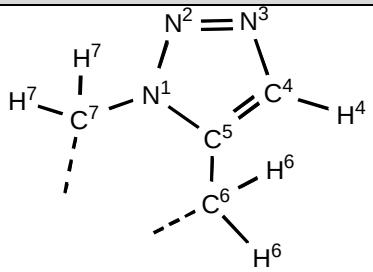 1,5-disubstituted 1,2,3-triazole	N^1	N/
	N^2	N(
	N^3	N)
	C^4	C/
	C^5	C(
	C^6	C2
	C^7	C2
	H^4	H4
	H^6	HC
	H^7	HC
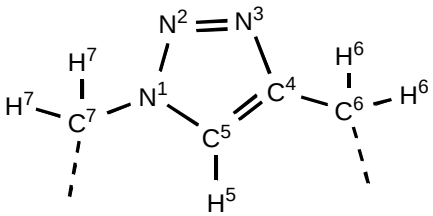 1,4-disubstituted 1,2,3-triazole	N^1	N$
	N^2	N%
	N^3	N&
	C^4	C$
	C^5	C%
	C^6	C2
	C^7	C2
	H^5	H4
	H^6	HC
	H^7	HC

Table S5 Bond parameters.

Atom1-Atom2	Force constant/(kcal/(mol×Å^2))	Equilibrium distance/Å
C$-C%	596.25000	1.377
C$-N&	596.25000	1.363
C2-C$	396.25000	1.509
C%-H4	458.75000	0.949
C%-N$	596.25000	1.366
N$-C2	632.25000	1.467
N&-N%	596.25000	1.293
N%-N$	596.25000	1.363
C(-C/	596.25000	1.377
C/-N)	596.25000	1.354
C2-C(	396.25000	1.479
C/-H4	458.75000	0.949
C(-N/	596.25000	1.365
N/-C2	632.25000	1.470
N)-N(	596.25000	1.322
N(-N/	596.25000	1.358
C2-h1	425.00000	1.093

Table S6 Angle parameters.

Atom1-Atom2-Atom3	Force constant/(kcal/(mol×rad^2))	Equilibrium angle/degrees
C2-C$-C%	373.02300	125.684
C2-C$-N&	373.02300	126.776
C$-C%-H4	95.500000	126.385
C$-C%-N$	373.02300	107.231
C$-N&-N%	373.02300	107.954
C%-N$-C2	373.02300	131.073
C%-C$-N&	373.02300	107.540
N&-N%-N$	373.02300	111.267
C%-N$-N%	373.02300	105.954

H4-C%-N$	95.500000	126.385
N%-N$-C2	373.02300	122.982
C$-C2-C1	64.700000	108.100
C$-C2-HC	47.200000	110.860
C1-C2-N$	65.800000	112.590
N$-C2-h1	49.900000	109.450
C2-C2-N$	65.800000	112.590
HC-C2-N$	49.900000	109.500
C2-C(-C/	373.02300	129.650
C2-C(-N/	373.02300	126.517
C(-C/-H4	95.500000	125.288
C(-C/-N)	373.02300	109.412
C/-N)-N(	373.02300	108.718
C(-N/-C2	373.02300	129.074
N)-N(-N/	373.02300	107.118
C(-N/-N(	373.02300	111.158
H4-C/-N)	95.500000	125.300
N(-N/-C2	373.02300	119.767
C/-C(-N/	373.02300	103.833
C(-C2-C1	64.700000	108.100
C(-C2-HC	47.200000	110.860
C1-C2-N/	65.800000	112.590
N/-C2-h1	49.900000	109.450
C2-C2-N/	65.800000	112.590
HC-C2-N/	49.900000	109.500
h1-C2-h1	39.200000	109.550
HC-C1-N	49.800000	109.500
C -C1-HC	47.200000	109.680
C1-C2-h1	46.400000	110.070
h1-C2-h1	39.200000	109.550
HC-C1-N	49.800000	109.500
C -C1-HC	47.200000	109.680

Table S7 Dihedral angle parameters.

Atom1-Atom2-Atom3-Atom4	Bond paths	Force constant/(kcal/mol)	Phase angle/degrees	periodicity
C2-C$-N&-N%	2	11.50000	180.00	2
C%-C$-N&-N%	2	11.50000	180.00	2
C2-C$-C%-N$	4	23.69000	180.00	2
C2-C$-C%-H4	4	23.69000	180.00	2
N&-C$-C%-N$	4	23.69000	180.00	2
N&-C$-C%-H4	4	23.69000	180.00	2
C$-C%-N$-C2	2	11.50000	180.00	2
C$-C%-N$-N%	2	11.50000	180.00	2
H4-C%-N$-C2	2	11.50000	180.00	2
H4-C%-N$-N%	2	11.50000	180.00	2
C2-N$-N%-N&	2	9.600	180.00	2
C%-N$-N%-N&	2	9.600	180.00	2
C$-N&-N%-N$	1	4.000	180.00	2
X -C$-C2-X	6	0.000	0.000	3
X -C2-N$-X	6	0.000	0.000	3
H4-C/-N)-N(	2	11.50000	180.00	2
C(-C/-N)-N(	2	11.50000	180.00	2
N/-C(-C/-H4	4	23.69000	180.00	2
C2-C(-C/-H4	4	23.69000	180.00	2
N/-C(-C/-N)	4	23.69000	180.00	2
C2-C(-C/-N)	4	23.69000	180.00	2
C/-C(-N/-C2	2	11.50000	180.00	2
C/-C(-N/-N(	2	11.50000	180.00	2
C2-C(-N/-C2	2	11.50000	180.00	2
C2-C(-N/-N(	2	11.50000	180.00	2
C2-N/-N(-N)	2	9.600	180.00	2
C(-N/-N(-N)	2	9.600	180.00	2
C/-N)-N(-N/	1	4.000	180.00	2
X -C2-C(-X	6	0.000	0.000	3
X -C2-N/-X	6	0.000	0.000	3